EXERCISE SCIENCE 운동과학
Vol.31, No. 3, August 2022: 392-402
https://doi.org/10.15857/ksep.2022.00276
ISSN(Print) : 1226-1726
ISSN(Online) : 2384-0544
ORIGINAL ARTICLE

Implantation of Decellularized Extracellular Matrix with Resistance Training Effectively Repairs a Volumetric Muscle Loss

Kwangjun Lee[1] MS, Kwang-Seok Hong[2] PhD, Wonil Park[2] PhD

[1]Department of Biomedical Sciences Program in Neuroscience, College of Medicine, Florida State University, Tallahassee, Florida, USA; [2]Department of Physical Education, College of Education, Chung-Ang University, Seoul, Korea

PURPOSE: Skeletal muscle has remarkable regenerative capacity in most minor injuries induced by mechanical laceration, overstretching, and toxins. However, volumetric muscle loss (VML) injury, a large volume of muscle loss beyond the self-repair capacity, causes functional disability and morphological deformities. This study investigated the effects of myofiber injection into a decellularized extracellular matrix (ECM) and resistance training (RT) on skeletal muscle regeneration following VML injury.

METHODS: 6-months-old male Fischer CDF rats and 2-months-old F344-Tg (UBC-EGFP) rats (myofiber donors) were used in this study. Approximately 20% of the mass of the lateral gastrocnemius (LGAS) was excised and replaced by ECM of similar dimensions. Thirty myofibers were injected into the injured region seven days post-injury. Ladder climbing (RT) was allowed 10 days post-defect surgery, and the rats were subjected to ladder climbing with a weight every third day for 6 weeks.

RESULTS: After 56 days of recovery and exercise training, the cross-sectional area (CSA) of intact muscle in the EXE group (5,104 ± 92 μm^2) increased significantly compared to that in the ECM (4,657 ± 79 μm^2) group. The number of blood vessels larger than 20 μm in diameter, capillaries excluded, showed a significant difference between the ECM+EXE (34.25 ± 4.2) and ECM (21.75 ± 3.89) groups. A significant reduction of fibrosis in the ECM+EXE (44.50 ± 1.6%) group was observed compared to the ECM (69.25 ± 1.9%) and ECM+FIB+EXE (63.00 ± 1.7%) groups. Moreover, the small muscle fiber area within the transplanted ECM was significantly larger in the ECM+EXE (1.37 ± 0.03 mm^2) than in both the ECM (0.49 ± 0.01 mm^2) and ECM+FIB (0.62 ± 0.01 mm^2) groups.

CONCLUSIONS: These data suggest that ECM transplantation with RT effectively repairs VML by enhancing hypertrophy, angiogenesis, and myofiber infiltration throughout the entire ECM.

Key words: Resistance training, Skeletal muscle regeneration, Satellite cells, Extracellular matrix, Angiogenesis

INTRODUCTION

Skeletal muscles, a bundle of multinucleated and contractile fibers, play a crucial role in the locomotion and structural support of the body [1,2]. Although adult myofibers are mitotically quiescent and their protein turnover rate is slow, skeletal muscles show a distinct self-repair capacity in most general injuries [3,4]. Satellite cells (SCs), adult stem cells, are primary sources of skeletal muscle repair. However, volumetric muscle loss (VML) becomes irreversible because fibrotic tissues occupy the injured area first, interrupting new myofiber growth [5]. Consequently, VML is characterized by severe damage to muscle mass, nerves, and blood vessels that cause functional deficits, cosmetic flaws, and a permanent handicap [6]. Surgical-free muscle transplantation is a typical current treatment for VML; however, functional and morphological repair to pre-injury conditions remains a big challenge.

The extracellular matrix (ECM) is a three-dimensional structure that is consisted of glycoproteins, heparin sulfate proteoglycans, glycosaminoglycans, and type IV collagen [7]. The ECM has a role in the functional and structural support of skeletal muscles [8]. The ECM also serves as a storage of growth factors, and the ECM binds to and releases growth factors directly. [9]. The ECM stores growth factors, including fibroblast growth factor (FGF), transforming growth factor-β (TGF-β),

Corresponding author: Wonil Park **Tel** +82-2-820-6371 **Fax** +82-2-812-0740 **E-mail** wonilpark01@cau.ac.kr
Received 11 Jul 2022 **Revised** 4 Aug 2022 **Accepted** 11 Aug 2022

hepatocyte growth factor (HGF), and vascular endothelial growth factor (VEGF), that significantly influence skeletal muscle growth and regeneration. Bidirectional interactions between ECM and these growth factors are involved in wound healing processes. Additionally, the chemokines released from degrading ECM response to skeletal muscle damage attract progenitor cells and stem cells to the injury region [10]. Because of the various roles of ECM in the wound healing process, both acellular ECM and biological scaffolds composed of ECM component proteins have been used to repair the tissues such as cardiac muscles, skeletal muscles, and abdominal skin [11]. Especially, acellular ECM scaffolds treated with progenitor cells have been extensively explored in VML injuries. The implantation of a homologous acellular ECM seeded with mesenchymal stem cell (MSC)s improved functional recovery after 42 days [12]. Implanting acellular ECM with myoblasts repaired abdominal wall defects [13], while homologous acellular ECM implantation only without myoblasts resulted in a large volume of fibrous scar tissues [14].

Satellite cells (SCs), adult skeletal muscle stem cells, are located between basal lamina and sarcolemma and are mitotically quiescent. Quiescent SCs are characterized by paired box 7, Pax7, which are crucial in SC development and lineage determination [15]. Upon exposure to a damaged environment, SCs start proliferating, referred to as myoblasts. The myoblasts enter the differentiation phase, and Myogenin and Myogenic factor 6 (Myf6) are highly expressed [16]. Myogenin and Myf6 are essential for the fusion of myoblasts, either themselves or with existing myofibers, to form myotubes. Newly regenerated small myofibers mature by increasing myotubes' size and expressing contractile proteins such as actin and myosin. Regenerated myofibers derived from donor SCs were investigated by observing a unique donor gene expression in the host cells. The green fluorescent protein expressing donor SCs fused with themselves or host myofibers. Even the donor SCs existed as SCs within the host myofibers through self-renewal [17,18]. Even though SCs are primary resources contributing to skeletal muscle regeneration, transplantation of enzymatically dissociated SCs often fails to complete muscle regeneration. Because the donor SCs are limited to migration and donor-host histocompatibility, resulting in early death in the host tissues. Therefore, freshly isolated single myofiber transplantation is an alternative treatment for delivering undamaged SCs to the injured host skeletal muscles. SC delivery via individual single myofiber transplantation not only maintains SC stemness by maintaining the original niche but also increases the survival ratio of donor SCs. A single donor myofiber transplantation promoted muscle hypertrophy, not hyperplasia. Transplantation of a single myofiber containing only 7-20 SCs generated more than 100 new myofibers containing 25,000-30,000 myonuclei [17]. Single fiber transplantation also increased contractile properties such as tetanic force production. Moreover, donor fiber-derived SCs from a young aged mouse remain permanently in the host muscle, preventing age-related skeletal muscle mass reduction [19].

Resistance training (RT) heavily influences the functional properties of skeletal muscle by modifying the structure, mass, and type of myofibers [20,21]. RT-induced metabolic stress and mechanical tension promoted the release of growth factors [22]. RT potentially induced large muscle mass and high contractile force by increasing CSA and modulating neuromuscular junctions [23]. Moreover, resistance and endurance training triggered angiogenesis and vascularization. VML patients treated with surgically placed ECM and custom-designed RT improved about 25 and 220% in force generation and functional tasks.

Vascularization is an inevitable concern in tissue engineering and tissue regeneration to provide nutrients and oxygen efficiently [24]. New myofiber formation should be synchronized with vascularization and innervation due to the role of blood vessels and nerves. Blood vessels supply nutrients and oxygen, and nerves transmit force. Transplantation of $CD34^{+}/45^{-}$ (SK-34) muscle-derived stem cells regenerated myofibers, blood vessels, and nerves resulting in a recovery of skeletal muscle mass and functional properties [25]. Innervation plays a vital role in characterizing morphological and functional skeletal muscle properties. Denervated skeletal muscle continued the path of degeneration due to a failure of neuromuscular junctions resulting in atrophy and tissue necrosis [26]. The role of neurotrophic factors, nerve growth factor (NGF), neurotrophin-3 (NT-3), and brain-derived neurotrophic factor (BDNF) in skeletal muscle regeneration has been widely studied. NGF is essential for the survival and growth of neurons. Phenotypic characterization of NGF knockout mice described an accumulation of cell death and muscle dystrophy [27]. Muscle-derived stem cells treated with NGF enhanced stem cell engraftment efficiency [28]. Since denervation results in adverse effects on skeletal muscle function and morphology, skeletal muscle regeneration following VML should accompany vascularization and innervation. Previous VML studies reported incomplete regeneration of skeletal muscle in the middle of the ECM compared to the top and bottom regions because of insufficient vascularization [12].

Therefore, this study aimed to determine the efficiency of skeletal muscle regeneration with supporting components, blood vessels, and nerves in the middle region of transplanted ECM via single fiber injection with RT.

METHODS

1. Animals

Male fischer 344 rats (Charles River Laboratories; Wilmington, MA), about 400 g of weight, were used in this study. F344-Tg (UBC-EGFP) was used for a myofiber donor. We used the rat to quantify regenerated myofibers from the donor SCs. Donor myofibers express the enhanced green fluorescent protein gene under the control of the human ubiquitin-C promoter. Animals were housed in a 12-hour light/dark cycle room and given ad-libitum access to food and water. A total of 32 rats were used for the study. They were randomly assigned to one of four groups (n = 8). Functional recovery was evaluated after 56 days from the initial defect surgery. All experimental procedures were conducted under Institutional Animal Care and Use Committee (IACUC) guidelines (AUP-2015-00008).

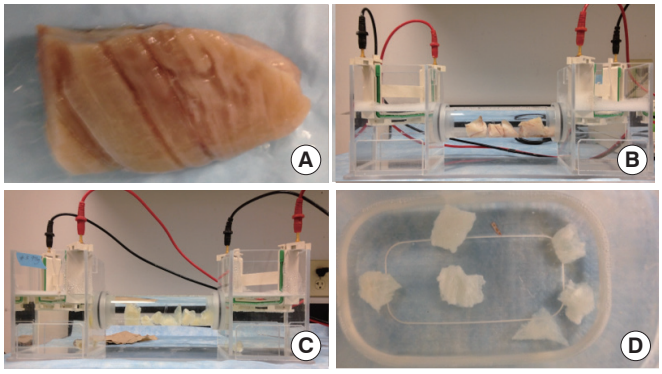

Fig. 1. Decellularization procedures using an electrophoresis system. (A) Fat and connective tissues were excised from the porcine muscle and cut into small pieces. (B) The tissues were placed in the electrophoresis machine with tris base, glycine, and SDS solution at a constant voltage of 60 V for 24 hours. (C) The electrophoresis process was repeated until all cellular materials were eliminated and the tissues became transparent. (D) The decellularized ECMs were placed in sterile PBS and exposed to ultraviolet light overnight until they were used for implantation.

2. ECM decellularization

Fat and connective tissues were excised from muscles and cut into small pieces. Deionized water (dH_2O) was injected throughout the whole muscles, and the muscles were placed in dH_2O for 2 hours to allow cellular swelling and rupture. Phosphate buffered saline (PBS) was injected throughout the entire muscles, and the muscles were placed in PBS for 2 hours. 0.25% Trypsin-EDTA (Gibco® Life Technologies; Burlington, ON, CA, USA) was injected throughout the whole muscles, and the muscles were placed in an oven for 45 minutes at 37°C. The tissues were then placed in glycerol (Fisher; Pittsburgh, PA, USA), disodium ethylenediaminetetraacetate dehydrate (EDTA) (Bio-Rad Laboratories; Hercules, CA, USA), deoxycholic acid (Fisher; Pittsburgh, PA, USA), and sodium dodecyl sulfate (SDS) (Sigma-Aldrich; St. Louis, MO, USA) solution for 48 hours. The tissues were placed in the electrophoresis machine with Tris base (Fisher; Pittsburgh, PA, USA), Glycine (Fisher; Pittsburgh, PA, USA), and SDS (Sigma-Aldrich; St. Louis, MO, USA) solution at a constant voltage of 60 V for 24 hours. 2% SDS was injected through the muscles, and the muscles were placed in SDS for 6 hours. The electrophoresis process was repeated until all cellular materials were eliminated. The ECM was rinsed in dH_2O until the water looked clear. The ECM was placed in sterile PBS (Invitrogen; Carlsbad, CA, USA) 1% antibiotic-antimycotic (Sigma-Aldrich; St. Louis, MO) (1% AA) overnight on a shaker. Next, the ECM was placed in 70% ethanol for 4 hours, subsequently placed in PBS 1% AA, and exposed to ultraviolet light overnight. Decellularized ECMs were stored at 4°C in sterile PBS with 1% AA until use in implantation. Fig. 1 represents the procedures of ECM decellularization.

3. VML creation & ECM implantation

Prior to VML surgery, a total of 32 animals were randomly assigned to one of four experimental groups: implantation of the ECM (ECM), implantation of the ECM followed by myofiber injection (ECM+FIB), implantation of the ECM followed by RT (ECM+EXE), and implantation of the ECM followed by myofiber injection and RT (ECM+FIB+EXE). All animals underwent removal of about 20% of muscle mass from the lateral gastrocnemius (LGAS). A piece of the exact dimensions of ECM was transplanted immediately, and myofibers were injected seven days later, as described by Collins [17]. All surgeries were conducted with aseptic tools while rats were anesthetized with 2-2.5% isoflurane gas. The rats were on a heating pad during the VML surgery. Briefly, a two-centimeter incision was made along the lateral side of the right lower leg, parallel with the tibia. The lateral portion of the LGAS was exposed by separating the biceps femoris. The soleus was gently separated from the LGAS by blunt forceps. A metal plate was placed between the soleus and the LGAS to prevent injury to the soleus upon creating the LGAS defect. Two #9 scalpel blades separated 1 cm by a spacer were used to create a similar defect shape for all animals. Approximately 1.0 × 1.0 cm full-thickness with 20% of the mass of the LGAS was excised. Immediately after the following defect, an ECM was prepared to the exact dimension of the excised muscle and implanted at the injury site us-

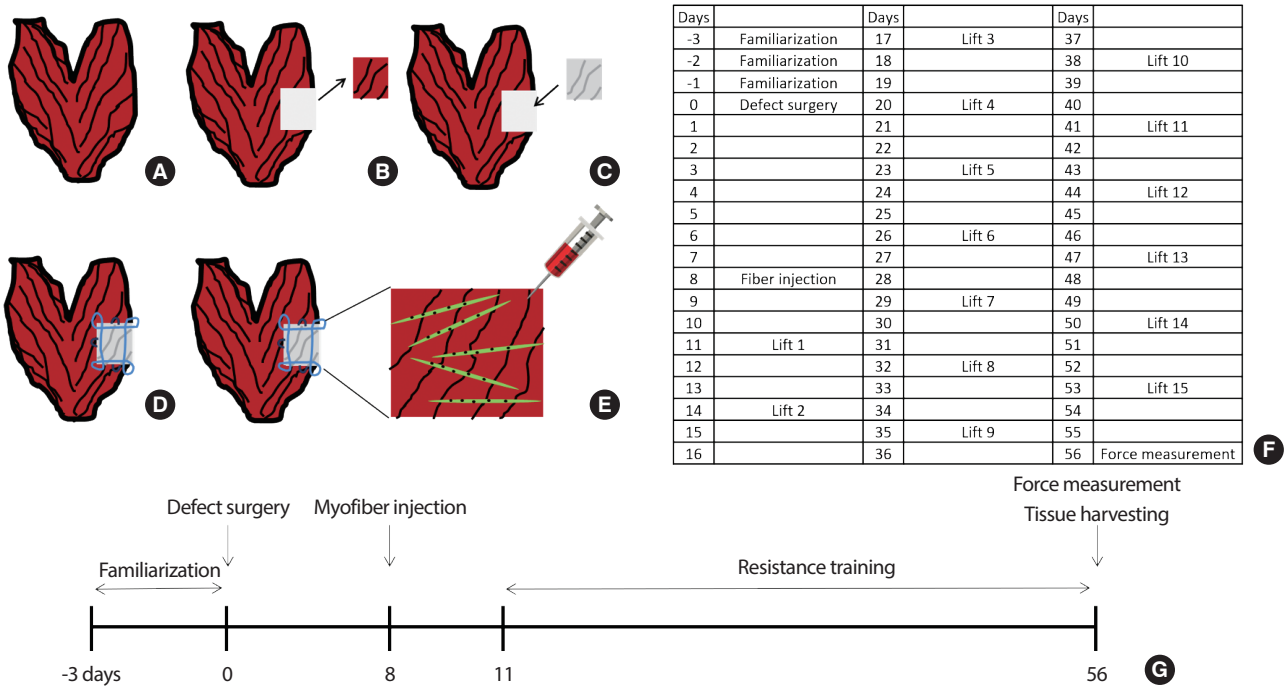

Days		Days		Days	
-3	Familiarization	17	Lift 3	37	
-2	Familiarization	18		38	Lift 10
-1	Familiarization	19		39	
0	Defect surgery	20	Lift 4	40	
1		21		41	Lift 11
2		22		42	
3		23	Lift 5	43	
4		24		44	Lift 12
5		25		45	
6		26	Lift 6	46	
7		27		47	Lift 13
8	Fiber injection	28		48	
9		29	Lift 7	49	
10		30		50	Lift 14
11	Lift 1	31		51	
12		32	Lift 8	52	
13		33		53	Lift 15
14	Lift 2	34		54	
15		35	Lift 9	55	
16		36		56	Force measurement

Fig. 2. Defect surgery and RT protocol. (A) Description of intact lateral gastrocnemius (LGAS). (B) About 20% of muscle mass from the LGAS was excised. (C) A piece of the exact dimensions of ECM was transplanted immediately at the injury site. (D) The ECM was sutured tightly by using a modified Kessler stitch. The suture was also a marker for a border of the defected muscle. (E) GFP expressing myofibers were injected 7 days after defect surgery. (F) RT started at 10 days post defect surgery. The rats climbed a ladder every third day for 6 weeks. (G) Description of experimental design.

ing a non-absorbable 5-0 polypropylene (5-0 prolene; Ethicon) suture. The ECM was fixed with A modified Kessler's stitch with simple interrupted sutures on three borders. The sutures were used as markers to distinguish between original tissues and regenerating tissues for histological and immune-histological analysis [29]. The biceps femoris was closed using simple interrupted polypropylene sutures (5-0 prolene; Ethicon). The skin was sutured via a simple interrupted suture (5-0 prolene; Ethicon) with the knot tied underneath the skin. Muscle loss injury and ECM implantation are shown in Fig. 2A-E. All rats were treated with buprenorphine (0.1 mg/kg, subcutaneously) 1 hour before and every 24 hours thereafter for the first 3 days post-surgery.

4. Myofiber isolation

Extensor digitorum longus (EDL) was excised from a donor rat and immediately digested by filtered 1.5% Collagenase type I in DMEM for 2 hours at 37°C and 5% CO_2. EDL isolation protocol is well optimized; age, sex, different muscles, or conditions should be considered to isolate single myofibers. Since the purpose of single myofiber injection was just delivering SCs, we used EDL instead of LGAS. During digestion, EDL was gently shaken every 30 minutes. When single myofiber was detached from the EDL, EDL and single fibers were transferred to a pre-warmed Petri dish with DMEM. One hundred single myofibers were isolated by pipetting from each EDLs.

5. Treatment surgery

The animals underwent 7 days of recovery to mitigate inflammation and increase the injected myofibers' survival ratio. The original stitches were removed to expose and visualize the transplanted ECM. GFP-expressing myofibers were isolated from F344-Tg (UBC-EGFP). 30 myofibers were injected evenly through the entire injury area using a 28.5-gauge needle with saline (SAL). After fiber injection, the biceps femoris and skin were sutured as previously described.

6. Exercise protocol

Exercise treatment groups, ECM+EXE and ECM+FIB-EXE, began RT at 10 days post defect surgery. This time allowed ECM adhesion with the injury site and force transmission across the defect region [30]. The rats climbed a ladder every third day for 6 weeks. The ladder was 1m in height with 2 cm steps and inclined at 85%. They were familiarized with the ladder by climbing it three times for three days before surgery. The

weights were attached to the proximal tail. The initial weight attached to a rat was 50% of body weight. The animals were encouraged to climb the ladder by gently touching the tail and pushing them behind. When rats completed climbing the ladder, they were allowed to rest for 2 minutes in a simulated cage at the top of the ladder apparatus. The load was set at 50, 75, 90, and 100% of the maximum load from the previous session. When rats could climb with 100% of the weight, 30 g of weight was subsequently added until they failed to climb the ladder. The training plan and experimental design are depicted in Fig. 2F-G.

7. Histology analysis

The LGAS was sectioned into 10 μm thickness perpendicular to the LGAS orientation with a Leica CM1900 cryostat microtome (Leica Microsystems; Wetzlar, Germany) at -20°C. Hematoxylin and eosin (H&E) (Thermo Fisher Scientific) staining was performed to identify intact and regenerated fibers. Masson's trichrome (Polysicence) was used to distinguish between myofiber and fibrous connective tissues. The sections were mounted with a permount mounting medium (Fisher Scientific; Waltham, MA). The sections were visualized with a Nikon Diaphot microscope with an Optronix Microfire digital camera. Histological quantification of H&E was performed on each level with the 20× objective lens.

8. Immunohistochemical analysis

A series of 10 μm cross-sections were taken from the top, middle, and bottom regions of the LGAS muscle. In preparation for immunofluorescent identification, sections were fixed in acetone for 3 minutes. Afterward, they were washed in 1X PBS and blocked with 5% normal donkey serum in PBS containing 1% bovine serum albumin (BSA). Sections were first incubated with primary antibodies against PECAM-1 (1:20, mouse monoclonal) and neurofilament 200 (1:200, rabbit polyclonal). PECAM-1 was detected with donkey anti-mouse IgGTRITC fluorescein (1:100, λ=546 nm), and neurofilament 200 was detected with anti-rabbit-Alexa 488 (1:100, λ=495 nm). Finally, all sections were counterstained with DAPI (1:1,000, λ=425 nm) to identify nuclei. Following a final wash in PBS, the sections were mounted in Permount mounting medium (Fisher Scientific; Waltham, MA, USA).

9. Imaging and analysis

Immunofluorescence was visualized with a Leica DM LB2 fluorescence microscope and photographed with a Leica DFC340FX digital camera (Leica Microsystems; Wetzlar, Germany). At each level and within each region of the ECM, the number of nerves and vessels was counted using Image J. A percentage of regenerated skeletal muscle and fibrotic tissue area in the ECM area was calculated. A blood vessel was only counted if its lumen was greater than 20 μm in diameter.

10. Statistical analysis

The data were presented as mean and standard deviation (mean±SD). One-way analysis of variance (ANOVA) was used for the analysis of

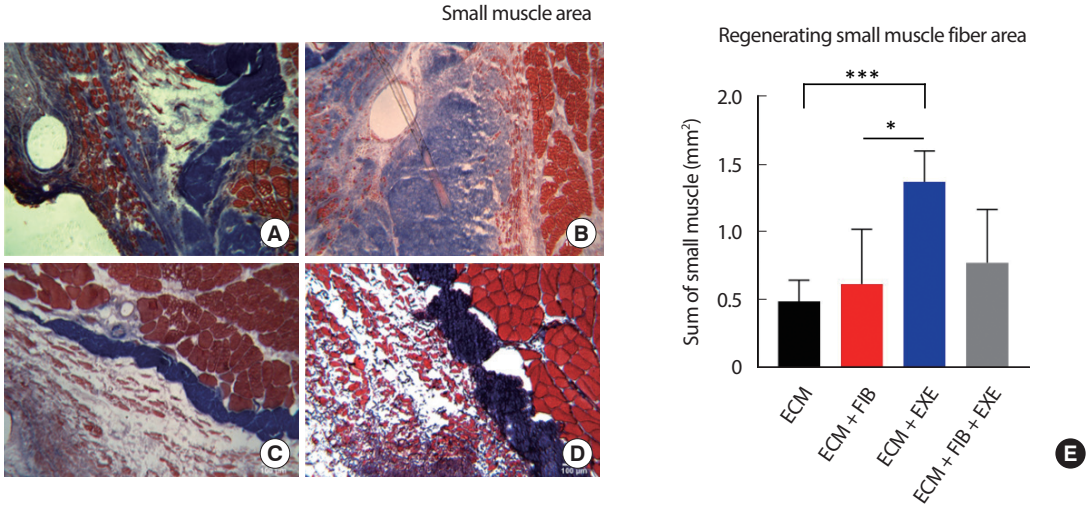

Fig. 3. Small myofiber density in the middle region of VML. Myofiber ingrowth was observed in the regenerating muscle area. Representative images of (A) ECM, (B) ECM+FIB, (C) ECM+EXE, and (D) ECM+FIB+EXE. Newly regenerating muscle small muscle fibers were stained red, and the fibrotic tissue area was stained blue. (E) Tissues were stained by Masson's trichome method, and regenerating small muscle fiber area was measured (n=4 in a group). *** and * indicate values that are different between the two groups. ***p<.001 and *p<.05 by an ANOVA with Tukey multiple-comparisons test.

group samples. Comparisons between the groups were made using Tukey's post hoc tests if it is significantly. Statistical significance was defined as $p < .05$.

RESULTS

1. Cross-sectional area

The average mass of the excised muscle was 176 ± 16 mg wet weight, approximately 20% of the total mass in the LGAS. The defect mass was approximated by initial body weight. The overall morphology of the VML LGAS was flattened compared to the LGAS from a contralateral limb. In previous work using homologous ECM transplantation, the morphology of the LGAS was well maintained following 56 days of recovery [12], but transplantation of porcine ECM was not retained its original round shape. The sum of the injured LGAS and initially removed muscle mass was 99.4 ± 1.7% of the contralateral LGAS. After 56 days of recovery, histological analysis demonstrated small myofibers were regenerated within the ECM (Fig. 3A-D). Quantified regenerating small muscle fiber area is shown in Fig. 3E. CSA was measured in the intact area to investigate compensatory hypertrophy and the effect of RT (Fig. 4A-D). The ECM+EXE (5,104 ± 92 μm^2) increased the CSA of intact muscle significantly compared to the ECM (4,657 ± 79 μm^2) (Fig. 4E-F). Newly regenerated myofibers at the border between the defect and ECM area were confirmed by central nuclei (Fig. 4G-J). Small and central nuclei containing myofibers represent that they are in the processes of regeneration and maturation. Centrally located nuclei in a large myofiber were mainly observed in the ECM+EXE and the ECM+FIB+EXE (Fig. 4I-J).

2. Neurogenesis and angiogenesis

Neurogenesis and angiogenesis within the transplanted ECM were measured by immunohistochemical analysis. Neurofilament staining revealed the presence of innervation at the border of regenerating area filled with central nuclei myofibers (Fig. 5A-D). However, nerves were not detected in the peripheral regions where no mature myofibers existed. Quantifying the total number of nerves throughout the area showed no significant differences between the experimental groups (Fig. 5E). Nerve CSA was measured and evaluated by size distribution. The small size of

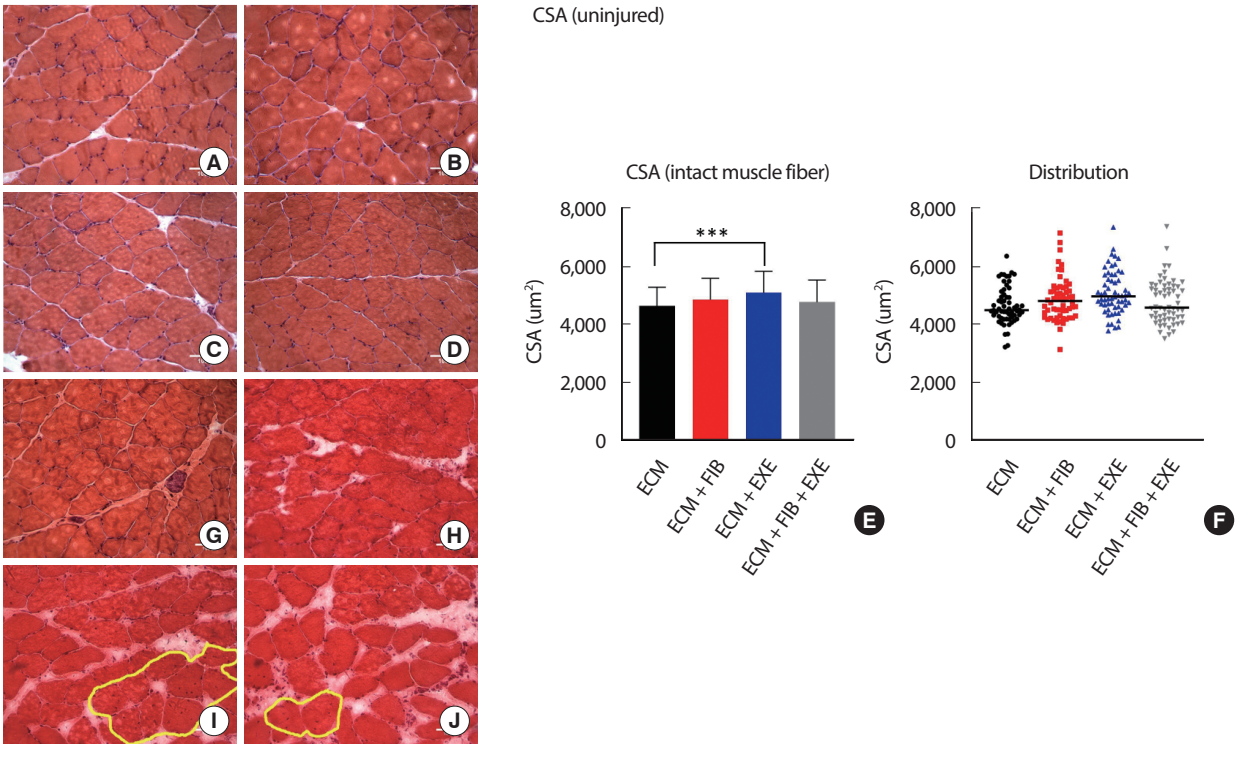

Fig. 4. CSA of uninjured muscle in the middle region of VML. Intact muscle hypertrophy was observed in the ECM+EXE. Representative images of (A) ECM, (B) ECM+FIB, (C) ECM+EXE, and (D) ECM+FIB+EXE. (E and F) Tissues were stained with hematoxylin and eosin, and CSA was measured (n = 4 *15 sections in a group) *** indicates values that are different between the two groups. ***p<.001 by an ANOVA with Tukey multiple-comparisons test. Centrally located nuclei in a large myofiber were mainly observed at the border between intact and injured muscle. Representative images of (G) ECM, (H) ECM+FIB, (I) ECM+EXE, and (J) ECM+FIB+EXE.

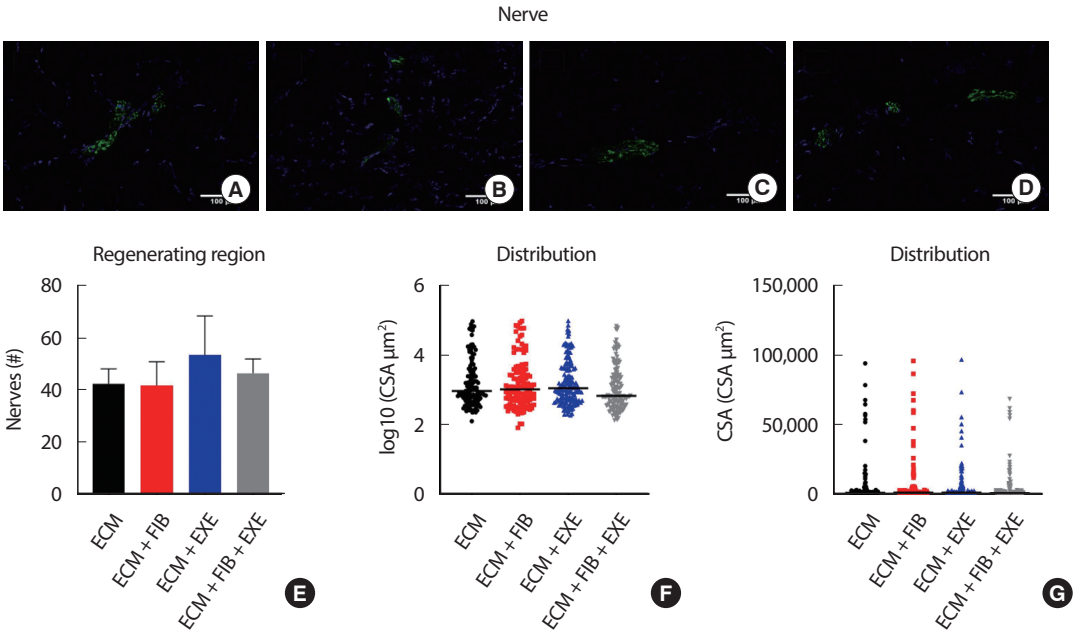

Fig. 5. Neurogenesis at the border between the intact and injured region of VML. Innervation was observed at the border of regenerating area filled with central nuclei myofibers. Representative images of (A) ECM, (B) ECM+FIB, (C) ECM+EXE, and (D) ECM+FIB+EXE. Neurons were identified by neurofilament 200 (GFP), and nuclei were stained by DAPI (blue) staining (n = 4 *15 sections in a group). (E) The total number of nerves was counted, and (F and G) nerve CSA was measured.

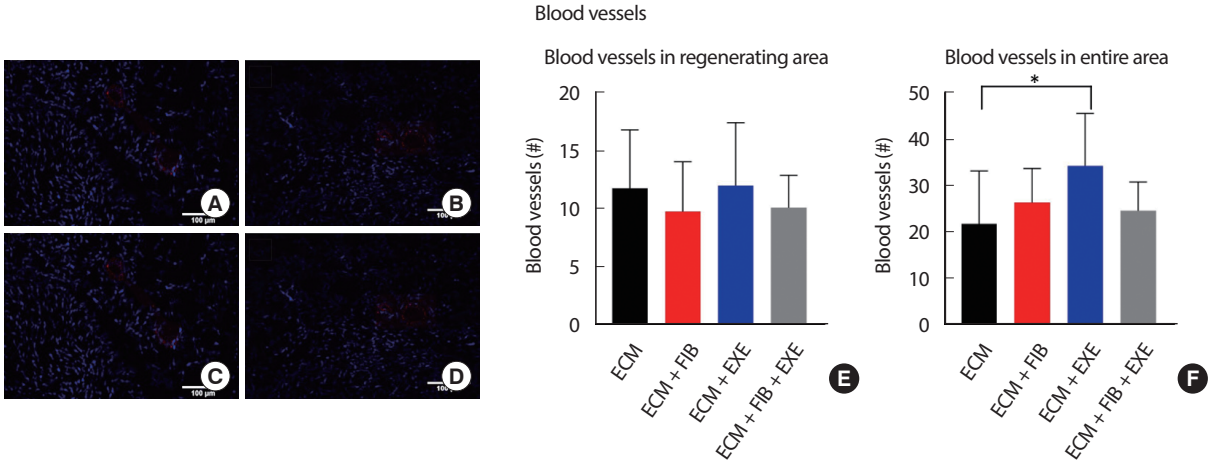

Fig. 6. Angiogenesis in the middle region of VML. Vascularization was observed in the regenerating region. Representative images of (A) ECM, (B) ECM+FIB, (C) ECM+EXE, and (D) ECM+FIB+EXE. Blood vessels were identified by PECAM-1 (TRITC), and nuclei were stained by DAPI (blue) staining. (E and F) The total number of blood vessels larger than 20 um in diameter was counted in the regenerating region (E) (n = 4 *15 sections in a group), and the entire region (F) (n = 4 *15 sections in a group). *indicate values that are different between two groups. *p<.05 by an ANOVA with Tukey multiple-comparisons test.

nerves, less than 1,000 μm², was dominant in all groups (Fig. 5F-G). PECAM staining showed angiogenesis at the border of regenerating area and in the middle region of the ECM filled with small myofibers (Fig. 6A-D). While the number of blood vessels in the regenerating area was not remarkably different among all groups (Fig. 6E), quantification of the number of blood vessels larger than 20 μm in the entire area showed a significant difference only in the ECM+EXE (34.25 ± 4.2) compared to the ECM (21.75 ± 3.89) (Fig. 6F). Although the ECM+EXE group tended to regenerate more blood vessels and nerves in the ECM region than the other groups, this difference was not significant (Figs. 5E, 6). In previous research, the middle region of ECM failed to repair blood vessels and myofibers compared to the top and bottom regions [12].

https://doi.org/10.15857/ksep.2022.00276

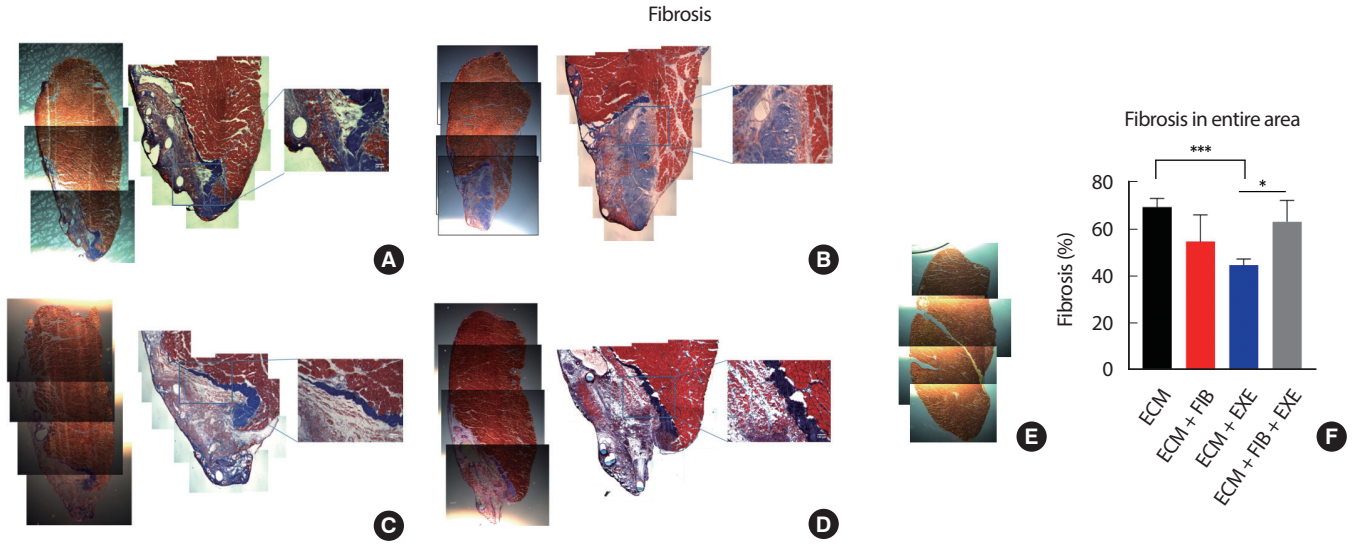

Fig. 7. Fibrosis in the middle region of VML. Fibrosis was observed in the regenerating region. Representative images of (A) ECM, (B) ECM+FIB, (C) ECM+EXE, (D) ECM+FIB+EXE, and (E) contralateral LGAS. (F) Fibrous connective tissues were measured by Masson's trichrome staining (Blue) (n=4 in a group). *** and * indicate values that are different between the two groups. ***$p<.001$ and *$p<.05$ by an ANOVA with Tukey multiple-comparisons test.

3. Fibrosis and newly regenerated small muscle fibers

Fibrous connective tissues were measured by Masson's trichrome staining. A significant attenuation of connective tissue area in the ECM+EXE (44.50±1.6%) was observed compared to ECM (69.25±1.9%) and ECM+FIB+EXE (63.00±1.7%) (Fig. 7A-D). Moreover, the small muscle fiber area within the transplanted ECM was significantly higher in the ECM+EXE group (1.37±0.032 mm^2) than in both ECM (0.49±0.011 mm^2) and ECM+FIB groups (0.62±0.015 mm^2) (Fig. 3A-D).

DISCUSSION

The large volume of skeletal muscle loss results in functional deficits, cosmetic flaws, and a permanent handicap. Moreover, associated psychological distress ensues from functional deficits and cosmetic flows accompanied by traumatic injuries. Current therapies improve myofiber infiltration and functional properties but fail to prevent fibrosis and improve angiogenesis and myofiber infiltration into the middle region of the ECM. Therefore, developing a therapy that can improve myofiber infiltration through entire regions of the transplanted ECM is imperative.

This study tested the combined effects of myofiber injection and RT on a VML injury. The results showed only the ECM+EXE positively affected skeletal muscle regeneration after 8 weeks of recovery. The ECM+EXE group significantly increased 15.7% mass recovery compared to the ECM group. RT increased muscle protein synthesis ratio, muscle mass, and contractile properties. RT by ladder-climbing stimulated several muscle groups, including the soleus, plantaris, and gastrocnemius. Ladder climbing training resulted in a 5-26% increase in muscle mass [31]. Previous research in our lab showed that 8 weeks of ladder climbing increased the mass by 23% and 14% of tetanic tension in the flexor hallucis longus muscle.

Moreover, muscle hypertrophy induced by 6 weeks of ladder climbing in VML injured LGAS increased by 11% of the mass and 16% of tetanic force [32]. The RT protocol was maximal high intensity, and the weight was added until an individual rat failed to climb the ladder. ECM+EXE climbed the ladder with 25% heavier loading than ECM+FIB+EXE at the last training (812 mg vs. 684 mg, $p<.01$). Less mass recovery and a minor change of CSA in ECM+FIB+EXE might be due to the lower exercise intensity compared to ECM+EXE. An additional surgery and recovery period after the myofiber injection attenuated exercise intensity in the early training period in the ECM+FIB+EXE. Although the ECM+FIB did not significantly improve, it prevented 15.2% fibrosis and enhanced 12.1% of small muscle regeneration compared to the ECM group. The GFP expressing donor SCs from single fiber injection fused and formed new myofibers in BaCl2 or cardiotoxin-induced skeletal muscle injuries [19]. Still, the number of GFP expressing myofibers was too low to analyze after 56 days post-injection in our VML model. Since transplanted decellularized ECM did not contain a neurovascular supply, donor SCs did not survive. The timing of donor stem cell injection should coordinate with vascularization and innervation in VML.

The transmission of nerve impulses causes skeletal muscle contraction. Innervation is vital in functional morphological skeletal muscle maintenance. Since denervation results in adverse effects on the muscle, it is essential that regenerating muscle fibers should accompany innervation in a VML injury. RT not only increases CSA and force generation but also affects neural plasticity on skeletal muscle. A 12-weeks of high RT slowly attenuated neuromuscular diseases [33], and RT induced a robust elevation of circulating BDNF [34]. Also, previous studies in our lab revealed that the ECM could be a scaffold supporting myofibers' growth and infiltration and blood vessels. Therefore, we postulate that RT can trigger innervation into ECM in a VML rat. In this experiment, ECM+EXE and ECM+FIB+EXE regenerated more nerves, but the difference was insignificant. Innervation only occurred in regenerating areas containing the mature size of the myofiber (Fig. 5A-D). Neurofilament staining failed to detect nerve like-structures in the regenerated small myofibers or connective tissue regions because innervation was the last step in the skeletal muscle regeneration process that affected myofiber maturation and functional recovery.

Blood vessels supply nutrients and oxygen to muscle tissues. In previous research in our lab, transplantation of ECM alone or with mesenchymal stem cells increased blood vessel density, not in the middle region. It means that the transplanted ECM can be a scaffold for angiogenesis. In this study, the ECM+EXE contained a significantly higher number of blood vessels than the ECM in the regenerating and entire areas. Resistance and endurance training triggered angiogenesis and vascularization [35,36]. Exercise training increased capillary density by activating VEGF [37] and endothelial progenitor cells [38]. RT also increased capillary density per fiber [39].

The remarkable finding in this study was that the ECM+EXE prevented fibrosis and promoted myogenesis in the middle region of the ECM. A repair of VML injury with only ECM implantation resulted in an incomplete recovery associated with functional loss and insufficient myofiber infiltration into the middle region of ECM [40]. Although the implanted ECM bridged the gap well, the infiltrating myofibers and blood vessels were only limited to the top and bottom regions closed to the uninjured muscle. RT influenced ECM remodeling and activated SC proliferation [41]. Continuous RT every three days could keep triggering the proliferation of SC, which helped myofiber infiltration into the middle region of the ECM.

The combined treatments of RT and single fiber injection did not have an additive effect. Even though a significant difference was not found between the ECM+EXE and ECM+EXE+INJ, the ECM+EXE recovered more LGAS muscle mass. The ECM+EXE recovered 87.6% of the LGAS mass, while the EXE+INJ groups recovered only 75.2% of the LGAS mass. After 6 weeks of RT, the ECM+EXE group climbed the ladder with 227% body mass, while the EXE+INJ group climbed the ladder with 187% body mass. The ECM+EXE significantly lifted more weight compared to the ECM+EXE+INJ. EXE+INJ receives surgeries twice, a defect surgery and a surgery for fiber injection, which may cause additional damage. Also, long-term RT needs to be examined because 56 days of recovery was not long enough to complete muscle regeneration in a 20% mass of severe VML injury. Small myofibers were still growing in the entire region of the ECM after 56 days of recovery.

CONCLUSION

In summary, the study proved the therapeutic potential for a continuous RT following ECM implantation. RT significantly affected histological and morphological recovery over ECM implantation alone. Different levels of RT intensity could affect skeletal muscle regeneration and functional properties. Donor single myofibers failed to survive and fuse to myofiber efficiently in severe VML. Myofiber injection into Pre-vascularized ECM is necessary to improve the survival ratio of donor stem cells.

CONFLICT OF INTEREST

The authors have no conflicts of interest to disclose.

AUTHOR CONTRIBUTIONS

Conceptualization: K Lee; Data curation: K Hong; Formal analysis: K Lee, K Hong; Funding acquisition: K Hong, W Park; Methodology: K Lee, W Park; Project administration: K Lee, W Park; Visualization: K Lee, K Hong; Writing-original draft: K Lee; Writing-review & editing: K Lee, K Hong, W Park.

ORCID

Kwangjun Lee https://orcid.org/0000-0002-7966-6846
Kwang-Seok Hong https://orcid.org/0000-0003-4691-5807
Wonil Park https://orcid.org/0000-0002-1623-6398

REFERENCES

1. Huard J, Li Y, Fu FH. Muscle injuries and repair: current trends in research. JBJS. 2002;84(5):822-32.
2. J Juhas M, Bursac N. Engineering skeletal muscle repair. COBIOT. 2013;24(5):880-6.
3. Rose AJ, Richter EA. Regulatory mechanisms of skeletal muscle protein turnover during exercise. J Appl Physiol. 2009;106(5):1702-11.
4. AdamsGR. Invited Review: Autocrine/paracrine IGF-I and skeletal muscle adaptation. J Appl Physiol. 2002;93(3):1159-67.
5. Greising SM, Rivera JC, Goldman SM, Watts A, Aguilar CA, et al. Unwavering pathobiology of volumetric muscle loss injury. Sci Rep. 2017;7(1):1-14.
6. Grogan BF, Hsu JR. Skeletal Trauma Research Consortium. Volumetric muscle loss. J Am Acad Orthop Surg. 2011;19:S35-7.
7. Theocharis AD, Skandalis SS, Gialeli C, Karamanos NK. Extracellular matrix structure. Adv Drug Deliv Rev. 2016;97:4-27.
8. Clark KA, McElhinny AS, Beckerle MC, Gregorio CC. Striated muscle cytoarchitecture: an intricate web of form and function. Annu Rev Cell Dev Biol. 2002;18(1):637-706.
9. Schultz GS, Wysocki A. Interactions between extracellular matrix and growth factors in wound healing. Wound Repair Regen. 2009;17(2):153-62.
10. Beattie AJ, Gilbert TW, Guyot JP, Yates AJ, Badylak SF. Chemoattraction of progenitor cells by remodeling extracellular matrix scaffolds. Tissue Eng Part A. 2009;15(5):1119-25.
11. Badylak S, Geddes L, Obermiller J. Extracellular matrix for myocardial repair in The heart surgery forum. Carden Jennings. 2003.
12. Merritt EK. Repair of traumatic skeletal muscle injury with bone-marrow-derived mesenchymal stem cells seeded on extracellular matrix. Tissue Eng Part A. 2010;16(9):2871-81.
13. Coppi PD. Myoblast-acellular skeletal muscle matrix constructs guarantee a long-term repair of experimental full-thickness abdominal wall defects. Tissue Eng. 2006;12(7):1929-36.
14. Conconi MT. Homologous muscle acellular matrix seeded with autologous myoblasts as a tissue-engineering approach to abdominal wall-defect repair. Biomaterials. 2005;26(15):2567-74.
15. Allen RE. Hepatocyte growth factor activates quiescent skeletal muscle satellite cells in vitro. J Cell Physiol. 1995;165(2):307-12.
16. Grounds MD. Identification of skeletal muscle precursor cells in vivo by use of MyoD1 and myogenin probes. Cell Tissue Res. 1992;267(1):99-104.
17. Collins CA. Stem cell function, self-renewal, and behavioral heterogeneity of cells from the adult muscle satellite cell niche. Cell. 2005;122(2):289-301.
18. Sacco A. Self-renewal and expansion of single transplanted muscle stem cells. Nature. 2008;456(7221):502-6.
19. Hall JK. Prevention of muscle aging by myofiber-associated satellite cell transplantation. Sci Transl Med. 2010;2(57):57ra83.
20. Adams GR. Skeletal muscle myosin heavy chain composition and resistance training. J Appl Physiol. 1993;74(2):911-5.
21. Lüthi J. Structural changes in skeletal muscle tissue with heavy-resistance exercise. Int J Sports Med. 1986;7(03):123-7.
22. Borst SE. Effects of resistance training on insulin-like growth factor-I and IGF binding proteins. MSSE. 2001;33(4):648-53.
23. Deschenes MR. Effects of resistance training on neuromuscular junction morphology. Muscle & Nerve. 2000;23(10):1576-81.
24. Li X. Effects of hypoxia on proliferation and differentiation of myoblasts. Med. Hypotheses. 2007;69(3):629-36.
25. Tamaki T. Functional recovery of damaged skeletal muscle through synchronized vasculogenesis, myogenesis, and neurogenesis by muscle-derived stem cells. Circ Res. 2005;112(18):2857-66.
26. Järvinen TA. Muscle injuries biology and treatment. Am J Sports Med. 2005;33(5):745-64.
27. Ruberti F. Phenotypic knockout of nerve growth factor in adult transgenic mice reveals severe deficits in basal forebrain cholinergic neurons, cell death in the spleen, and skeletal muscle dystrophy. J Neurosci. 2000;20(7):2589-601.
28. Lavasani M. Nerve growth factor improves the muscle regeneration capacity of muscle stem cells in dystrophic muscle. Hum Gene Ther. 2006;17(2):180-92.
29. Kragh Jr JF. Epimysium and perimysium in suturing in skeletal muscle lacerations. J Trauma Acute Care Surg. 2005;59(1):209-12.
30. Kjær M. Role of extracellular matrix in adaptation of tendon and skeletal muscle to mechanical loading. Physiol Rev. 2004;84(2):649-98.
31. Hornberger Jr TA, Farrar RP. Physiological hypertrophy of the FHL muscle following 8 weeks of progressive resistance exercise in the rat. Can. J Appl Physiol. 2004;29(1):16-31.
32. Lee S. Viral expression of insulin-like growth factor-I enhances muscle hypertrophy in resistance-trained rats. J Appl Physiol. 2004;96(3):1097-104.
33. Kilmer DD. The effect of a high resistance exercise program in slowly

progressive neuromuscular disease. Arch Phys Med Rehabil. 1994;75 (5):560-3.
34. Yarrow JF. Training augments resistance exercise induced elevation of circulating brain derived neurotrophic factor (BDNF). Neurosci Lett. 2010;479(2):161-5.
35. Green H. Regulation of fiber size, oxidative potential, and capillarization in human muscle by resistance exercise. Am J Physiol Regul Integr Comp Physiol. 1999;276(2):R591-6.
36. Laughlin M, Roseguini B. Mechanisms for exercise training-induced increases in skeletal muscle blood flow capacity: differences with interval sprint training versus aerobic endurance training. J Physiol Pharmacol. 2008;59(Suppl 7):71.
37. Amaral SL, Papanek PE, Greene AS. Angiotensin II and VEGF are involved in angiogenesis induced by short-term exercise training. Am J Physiol Heart Circ Physiol AM J. 2001;281(3):H1163-9.
38. Laufs U. Physical training increases endothelial progenitor cells, inhibits neointima formation, and enhances angiogenesis. Circ. 2004;109(2): 220-6.
39. McCall G. Muscle fiber hypertrophy, hyperplasia, and capillary density in college men after resistance training. J Appl Physiol. 1996;81(5): 2004-12.
40. Merritt EK. Functional assessment of skeletal muscle regeneration utilizing homologous extracellular matrix as scaffolding. Tissue Eng Part A. 2010;16(4):1395-405.
41. Mackey A. Enhanced satellite cell proliferation with resistance training in elderly men and women. Scand J Med Sci Sports. 2007;17(1):34-42.